SPECTRAL ANALYSIS OF MICRO-BUNCHING INSTABILITIES USING FAST THz DETECTORS

J. L. Steinmann, E. Hertle, N. Hiller, V. Judin, A.-S. Müller, P. Schönfeldt, M. Schuh, P. Schütze,
Karlsruhe Institute of Technology (KIT), Karlsruhe, Germany
E. Bründermann[*], Ruhr-Universität Bochum (RUB), Bochum, Germany

Abstract

Micro-bunching instabilities occur at synchrotron light sources when the particle density rises due to compression of the electron bunches. They lead to powerful bursts of coherent synchrotron radiation (CSR) in the THz range at the cost of very unstable intensity and spectral properties, highly fluctuating on a millisecond time scale. For interferometry this changing source demands a long averaging time to achieve a reasonably high signal-to-noise ratio or balancing by the use of an additional reference detector. In this study we present measurements taken by a Martin-Puplett-interferometer in the bursting regime with ultra-fast THz-detectors.

INTRODUCTION

ANKA Synchrotron Radiation Facility

The "ANKA Synchrotron Radiation Facility" is a synchrotron light source located at the Karlsruhe Institute of Technology (KIT) that provides dedicated low-α_c operation in single- and multi-bunch mode to users since 2003 [1]. It is a 500 MHz ramping machine that can be operated between 500 MeV and 2.5 GeV. For stability reasons and to achieve the shortest bunches, low-α_c operation is mostly performed at 1.3 GeV. All experiments presented in this paper have been carried out at the ANKA-IR1 beamline, a dedicated edge radiation beamline [2].

Low-α_c Operation at ANKA

Since the zero-current bunch length is proportional to the square root of the momentum compaction factor α_c, the bunches can be squeezed by lowering the α_c-value via controlling the beam optics. Short bunches in the order of a few pico seconds create CSR for the long wavelengths in the THz regime. When the emitted electric fields of N electrons add up coherently, the radiated power scales with N^2. This leads to a power gain by a factor of N, compared to incoherent synchrotron radiation (ISR). Depending on the bunch current there are 10^8 to 10^{10} electrons in a bunch, which is very beneficial for all users performing experiments in the long wavelength spectral range.

The power gain is partially constrained, because the low frequencies in the microwave regime are shielded by the ANKA vacuum chamber of 32 mm height. The radiated spectrum of shielded CSR by a Gaussian bunch can be calculated [3]. The expected spectra for bunches of different length and a bunch current of 1 mA ($\hat{=}\ 2.3 \times 10^9$ electrons) in the ANKA vacuum chamber are shown in Fig. 1. The plot shows that for long bunches above 12 ps practically no CSR is observable. However, for shorter bunches an increase of radiated power by orders of magnitude is observed.

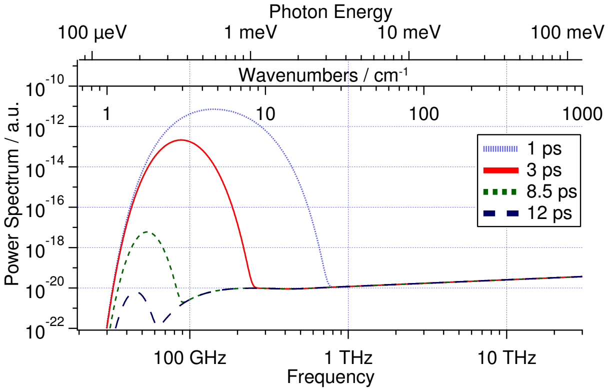

Figure 1: Calculated CSR Spectrum for Gaussian bunches with different bunch length. Low frequencies are shielded by the ANKA vacuum chamber of 32 mm height.

Micro-Bunching Instabilities at Low-α_c Operation

The bunch compression is limited by micro-bunching instabilities that occur at high particle densities. Commonly, ANKA is operated for users in low-α_c mode - for stability reasons - below the so-called bursting-threshold in the steady-state regime. In this regime the maximum bunch current for stable operation at a given bunch length is limited. However, the unstable bursting regime is of interest for several reasons: Future low emittance storage rings will be operated at low values of α_c and therefore might have to deal with micro-bunching instabilities. Micro-bunches emit higher frequencies than purely Gaussian-shaped bunches, and, therefore, can provide high power for experiments.

Unfortunately, the shape of the micro-bunches is unstable and the radiated power changes rapidly because of a changing spectrum. In Fig. 2 the intensity of a light pulse in the THz range is plotted over time. Each point represents the amplitude at one revolution. The amplitude of the pulse is bursting almost regularly depending on the bunch current.

FAST THz-DETECTORS

Most experiments use rather slow but sensitive detectors and average the underlying bursting signals. Also balanced detection, where a second detector balances out the instabilities, is used [4]. The frequency of the appearing intensity bursts corresponds to hundreds of Hertz and the needed averaging time is rather high, thus, the acquisition speed limited.

---

[*] on leave to KIT

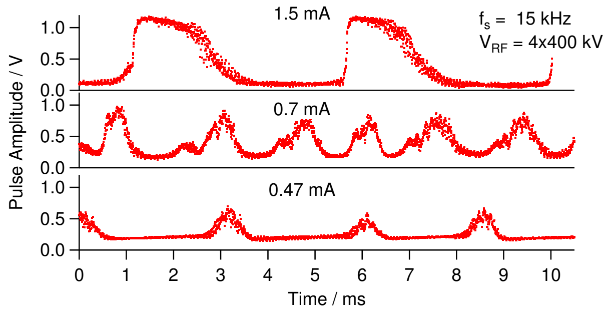

Figure 2: Detectors sensitive in the unstable part of the synchrotron spectrum observe a changing source power. Frequently occurring micro-bunches lead to intensity fluctuations, characteristic for different bunch charges.

The interest in time-resolved measurements makes the use of fast detectors and matched fast electronic readout mandatory. Slowly pulsing light sources such as the new linac-based THz light source at KIT named FLUTE [5], operating at a repetition rate of 10 Hz, and synchrotron operation in single-bunch mode can significantly benefit from faster detectors: The average power is low compared to the peak power, so that the signal-to-noise ratio (SNR) can be improved by orders of magnitude, if we measure only during the short light pulse interval and neglect the noise in-between.

Fast Schottky detectors have an adequate SNR even at room temperature when measuring high power pulses. We use ultra-wide-band quasi-optical zero-bias Schottky-barrier diode detectors from ACST [6]. These room temperature detectors are equipped with a log-spiral antenna to receive radiation between 50 GHz and 2 THz. Their speed is limited by an internal 4 GHz amplifier, which allows to resolve consecutive bunches at ANKA. The peak sensitivity of 450 V/W is reached at 70 GHz. The noise equivalent power (NEP) is sufficient to detect CSR in the bursting regime, but it is insufficient to measure ISR. In addition, the impulse response is linear.

Fast THz detectors are optimized for speed, but their frequency response is often not constant. We normalized the results by the detector's spectral sensitivity to minimize the effect of different detector responsivity and to allow comparison even during micro-bunching, which can alter the spectral intensity distribution significantly.

MARTIN-PUPLETT INTERFEROMETRY

Conventional beam splitters used in Michelson interferometers limit broadband measurements in the THz range, in contrast to a Martin-Puplett interferometer (MPI), which uses wire-grids as beam splitters that split the beam by polarization [7]. If the time resolution of the detector is faster than the time scales which correspond to the bursting frequencies, balancing would be desirable to compensate for the unstable source power.

The MPI provides two cross-polarized beams at different outputs that can be recorded simultaneously and give complementary interferograms (IFG), which can enable balancing. By calculating the difference interferogram of the horizontally I_H and vertically I_V polarized signals and normalization by the sum according to (1), small fluctuations can be damped and the signal-to-noise ratio improved [8].

$$I_B = \frac{I_H - I_V}{I_H + I_V} \qquad (1)$$

BURSTING STUDIES WITH MPI

Measurements have been done in step-scan and rapid-scan mode. While in step-scan mode the movable mirror is driven in small steps and data is taken at a stable position before moving to the next step, in rapid-scan mode the mirror moves continuously, allowing faster data acquisition. The experimental set-up is shown in Fig. 3. A polarizer ensures that linearly polarized light enters the interferometer. The beam is divided by a wire-grid beam splitter, reflected at rooftop mirrors and recombined again. Another wire-grid, mounted at 45 degrees, divides the horizontal and vertical polarized beam components to illuminate two Schottky detectors.

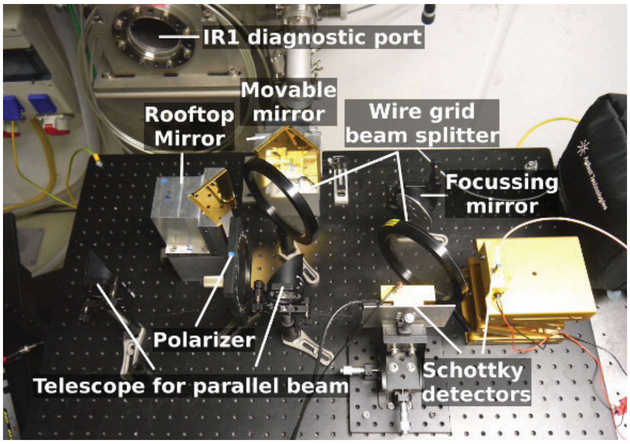

Figure 3: Set-up of the Martin-Puplett interferometer.

Interferometry in the bursting regime is very challenging. The repetition rate of the bursts is usually between 400 and 600 Hz. This means that the interferogram is taken over several bursts that overlay the interferogram and have to be compensated by balancing.

Step-Scan Mode

In step-scan mode data was recorded for several 100 ms for both Schottky diodes at every step. Fig. 4 shows the acquisition of the interferogram. First, a time signal at a mirror position is recorded while the amplitude of the pulse seen by the Schottky diode is measured every turn and recorded over time (Fig.4 top trace). The height of the burst depends on the form factor of the micro-bunches and is not easily predictable. This height of intensity fluctuations can't be fully compensated by balancing. We Fourier-transformed the raw signal and determined the amplitude of the main bursting frequency (usually around 500 Hz). This is used as a point for the interferogram corresponding to the current mirror position. Then the next point is measured. When the full interferogram is acquired, it is processed and Fourier-transformed as usual FTIR-interferograms [9] to get the spectrum.

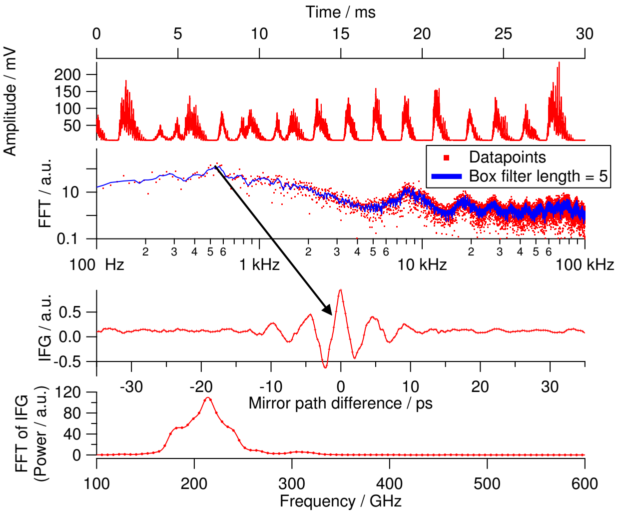

Figure 4: Process to get the interferogram (IFG) and spectrum during bursting in step-scan mode. For detailed explanation see text.

Rapid-Scan Mode

In rapid-scan mode, the interferogram is modulated by the bursts of radiation that lead to an unstable source power. Figure 5 shows a spectrum taken during bursting mode with the MPI using balancing detection to partially compensate for the unstable source power. In comparison, a spectrum at the same machine parameters was recorded using a commercial Michelson interferometer (Bruker GmbH, Germany) while averaging 16 scans.

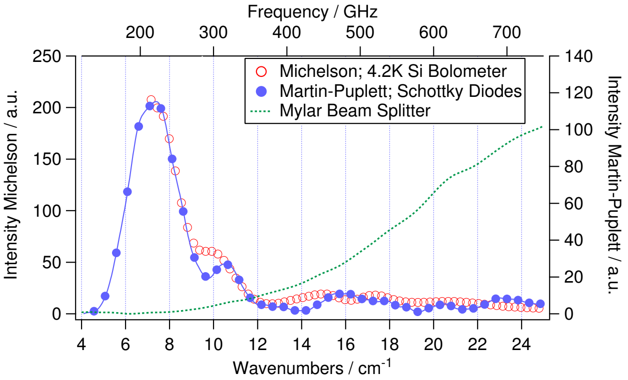

Figure 5: Spectra taken with Michelson and Martin-Puplett interferometer at the same beamline and machine settings. Both have been normalized by the beam splitter respective detector response function.

We used a $50\,\mu\mathrm{m}$ Mylar beam splitter and a 4.2 K Si bolometer at the Michelson interferometer and room temperature Schottky detectors at the MPI. The Mylar beam splitter has a limited bandwidth and a zero-pole at approx. 6 wavenumbers. For comparison, we normalized the spectra by the beam splitter transfer function, but left out the points of the zero-pole location.

The spectra are in good agreement, if we consider the low NEP of fast room temperature Schottky diodes compared to a slow and sensitive bolometer at 4.2 K. The bunch length for this measurement was 8.5 ps. The measured spectrum shows stronger damping for lower frequencies in comparison to the theoretical simulation (cf. Fig.1) due to a non-optimized THz transport in the ANKA-IR1 beamline. For this bunch length there is no stable CSR visible, only the radiation emitted by micro-bunching instabilities.

CONCLUSION AND OUTLOOK

We have shown that interferometry with fast THz detectors in the bursting regime is possible and can be used for spectroscopy. The emitted synchrotron radiation spectrum is changing faster than the available scan speed, so that a faster method is preferred to study micro-bunching instabilities. We will use balanced detection with ultra-fast THz detectors to balance out bursting instabilities on a bunch-by-bunch basis, which is feasible with the new KAPTURE system (KArlsruhe Pulse Taking and Ultrafast Readout Electronics) [10]. It enables us to continuously acquire the signal of up to 4 detectors for every bunch during every revolution. Signal balancing will be performed by an integrated FPGA that drives a balanced low frequency output with drastically improved signal-to-noise ratio, which is fed into the following signal processing unit, for example, a spectrometer software.

ACKNOWLEDGMENT

We would like to thank Y.-L. Mathis and his team from the ANKA Infrared-Group for excellent support at the beamlines. Also we acknowledge the fruitful discussions with, and support of, the ANKA THz group. This work is supported by the Helmholtz International School for Teratronics.

REFERENCES

[1] A.-S. Müller et al., ICFA Beam Dynamics Newsletter **57**, 154–165 (2012).

[2] Y.-L. Mathis et al., J. Biol. Phys., **29**, 313–318 (2003).

[3] A. Novokhatski, ICFA Beam Dynamics Newsletter **57**, 127-144 (2012).

[4] J. Barros et al., Rev. Sci. Instrum. **84**, 033102 (2013).

[5] M.J. Nasse et al., Rev. Sci. Instrum. **84**, 022705 (2013).

[6] C. Sydlo et al., Frequenz (2008).

[7] E. Bründermann et al., *Terahertz Techniques*, Springer Series in Optical Sciences, Vol. 151 (2012).

[8] L. Fröhlich, DESY-THESIS-2005-011 (2005).

[9] P. Griffiths, J.A. de Hasseth, *Fourier Transform Infrared Spectrometry* (2nd ed.), Wiley-Blackwell, (2007).

[10] M. Caselle et al., IPAC'14, Dresden, Germany, THPME113, *These Proceedings*.